Chemically Induced Conditional Rescue of the *Reduced Epidermal Fluorescence8* Mutant of Arabidopsis Reveals Rapid Restoration of Growth and Selective Turnover of Secondary Metabolite Pools[1][C][OPEN]

Jeong Im Kim, Peter N. Ciesielski, Bryon S. Donohoe, Clint Chapple, and Xu Li*

Department of Biochemistry, Purdue University, West Lafayette, Indiana 47907 (J.I.K., C.C.); Bioscience Center, National Renewable Energy Laboratory, Golden, Colorado 80401 (P.N.C., B.S.D.); Department of Plant and Microbial Biology, North Carolina State University, Raleigh, North Carolina 27695 (X.L.); and Plants for Human Health Institute, North Carolina State University, Kannapolis, North Carolina 28081 (X.L.)

The phenylpropanoid pathway is responsible for the biosynthesis of diverse and important secondary metabolites including lignin and flavonoids. The *reduced epidermal fluorescence8* (*ref8*) mutant of Arabidopsis (*Arabidopsis thaliana*), which is defective in a lignin biosynthetic enzyme *p*-coumaroyl shikimate 3′-hydroxylase (C3′H), exhibits severe dwarfism and sterility. To better understand the impact of perturbation of phenylpropanoid metabolism on plant growth, we generated a chemically inducible *C3′H* expression construct and transformed it into the *ref8* mutant. Application of dexamethasone to these plants greatly alleviates the dwarfism and sterility and substantially reverses the biochemical phenotypes of *ref8* plants, including the reduction of lignin content and hyperaccumulation of flavonoids and *p*-coumarate esters. Induction of *C3′H* expression at different developmental stages has distinct impacts on plant growth. Although early induction effectively restored the elongation of primary inflorescence stem, application to 7-week-old plants enabled them to produce new rosette inflorescence stems. Examination of hypocotyls of these plants revealed normal vasculature in the newly formed secondary xylem, presumably restoring water transport in the mutant. The *ref8* mutant accumulates higher levels of salicylic acid than the wild type, but depletion of this compound in *ref8* did not relieve the mutant's growth defects, suggesting that the hyperaccumulation of salicylic acid is unlikely to be responsible for dwarfism in this mutant.

Phenylpropanoids including flavonoids, hydroxycinnamate esters, and lignin have been shown to play important roles in many aspects of plant growth and development. Flavonoids are important for flower pigmentation and pollen viability in some species (Coe et al., 1981; Mo et al., 1992; Taylor and Jorgensen, 1992; Mol et al., 1998), and sinapate esters, a class of hydroxycinnamate esters found in Arabidopsis (*Arabidopsis thaliana*) and related members of the Brassicaceae, are important UV protectants (Landry et al., 1995). Lignin is a major component of the plant cell wall, where it confers mechanical strength to plants, and is important for the vascular system to conduct long-distance water transport. Reducing lignin content or manipulating its composition is of great interest in an applied context because of the polymer's negative impact on the utilization of cellulosic biomass for feed, paper manufacture, and biofuel production (Li et al., 2008).

The lignin biosynthetic pathway has been largely elucidated during the last two decades (for review, see Bonawitz and Chapple, 2010; Vanholme et al., 2013). In Arabidopsis and other species, down-regulation or mutation of genes and enzymes early in the pathway leads to drastic lignin reduction and a concomitant inhibition of plant growth. For example, knocking out four Phe ammonia-lyase genes (PAL) in Arabidopsis decreases lignin content by 75% and results in stunted and sterile plants (Rohde et al., 2004; Huang et al., 2010). Arabidopsis *reduced epidermal fluorescence3* (*ref3*) and *ref8* mutants, which are defective in cinnamate 4-hydroxylase (C4H) and *p*-coumaroyl shikimate 3′-hydroxylase (C3′H), respectively, as well as RNA interference (RNAi) plants in which hydroxycinnamoyl-CoA shikimate: hydroxycinnamoyl transferase (HCT) was suppressed, also display severe growth defects and sterility (Franke et al., 2002b; Hoffmann et al., 2004; Abdulrazzak et al., 2006; Besseau et al., 2007; Schilmiller et al., 2009; Li et al.,

[1] This work was supported by the Center for Direct Catalytic Conversion of Biomass to Biofuels, an Energy Frontier Research Center funded by the U.S. Department of Energy, Office of Science, Office of Basic Energy Sciences (award no. DE–SC0000997), and the Division of Chemical Sciences, Geosciences, and Biosciences, Office of Basic Energy Sciences of the U.S. Department of Energy (award no. DE–FG02–07ER15905).

* Address correspondence to sirius_li@ncsu.edu.

The author responsible for distribution of materials integral to the findings presented in this article in accordance with the policy described in the Instructions for Authors (www.plantphysiol.org) is: Xu Li (sirius_li@ncsu.edu).

[C] Some figures in this article are displayed in color online but in black and white in the print edition.

[OPEN] Articles can be viewed online without a subscription.

www.plantphysiol.org/cgi/doi/10.1104/pp.113.229393

2010). The association between lignin modification and plant growth reduction has also been reported in several other species, including poplar (*Populus* spp.), tobacco (*Nicotiana tabacum*), and alfalfa (*Medicago sativa*; Piquemal et al., 1998; Pinçon et al., 2001; O'Connell et al., 2002; Reddy et al., 2005; Leplé et al., 2007; Shadle et al., 2007). Despite its wide occurrence, it is not yet clear how the perturbation of phenylpropanoid metabolism influences plant growth and development (Bonawitz and Chapple, 2013). Considering the biological roles of lignin in providing mechanical strength and hydrophobicity in the vascular system, lignin deficiency may directly impact plant growth. Alternatively, various nonlignin phenylpropanoids are produced through the phenylpropanoid pathway, and deficiency or accumulation of those compounds may also contribute to the alteration of plant growth. For example, decreasing PAL activity by either suppressing *PAL* expression or applying PAL inhibitors resulted in reduced levels of salicylic acid (SA) and reduced systemic-acquired resistance to pathogens in tobacco and Arabidopsis (Mauch-Mani and Slusarenko, 1996; Pallas et al., 1996; Huang et al., 2010). Several Arabidopsis nonphenylpropanoid mutants containing increased SA content also display dwarfism (Bowling et al., 1994; Petersen et al., 2000; Li et al., 2001; Lee et al., 2007). These observations suggest a possible link between SA homeostasis and plant growth. A recent study showed that Arabidopsis plants with reduced *HCT* expression have elevated levels of SA and reducing the SA accumulation in these plants alleviated their dwarfism (Gallego-Giraldo et al., 2011). Some soluble phenylpropanoids such as dehydrodiconiferyl alcohol glycosides had been shown to have a cell division-promoting effect and therefore might also contribute to the growth defects of the plants in which the phenylpropanoid metabolism is perturbed (Binns et al., 1987; Lynn et al., 1987; Teutonico et al., 1991; Orr and Lynn, 1992).

To better understand how phenylpropanoid metabolism impacts plant growth and to probe secondary metabolite synthesis and turnover, we investigated temporal changes in lignification, plant growth, and phenylpropanoid levels in the Arabidopsis *ref8* mutant using a chemically inducible system. Here, we report that the ability of *C3′H* to restore growth of the *ref8* mutant depends on when it is activated during the development of the plants. Our data also revealed selective turnover of different phenylpropanoid metabolite pools upon *C3′H* induction. Finally, unlike a recent report of the importance of SA in HCT-RNAi-induced dwarfing, our results suggest that the accumulation of SA is unlikely to be the cause for growth inhibition in *ref8* plants.

RESULTS

Rescue of *ref8* by Chemically Induced Expression of *C3′H*

To investigate the relationship between metabolic changes in phenylpropanoid metabolism and plant growth and development, we generated transgenic Arabidopsis *ref8* mutant plants that express *C3′H* in a chemically inducible manner, designated as *ref8*^{pOpON}. We employed a stringent glucocorticoid-inducible system, pOpON, which has been shown to allow effective control of transgene expression in Arabidopsis by dexamethasone (dex) application (Craft et al., 2005; Wielopolska et al., 2005; Moore et al., 2006). To examine the dynamics of *C3′H* transgene transcript levels in response to dex application in the *ref8*^{pOpON} lines, quantitative reverse transcription (RT)-PCR was performed to monitor the relative expression levels of *C3′H* in three independent transgenic *ref8*^{pOpON} lines, *ref8*, and the wild type. As shown in Figure 1, whereas dex has little effect on *C3′H* expression in either the wild type or *ref8*, the *C3′H* transcript levels in the three *ref8*^{pOpON} lines were increased about 20-fold within 2 h of dex treatment. Because increased *C3′H* expression was relatively stable for at least 7 d without additional dex application, dex treatment at a frequency of once per week was deemed sufficient to maintain continuous expression of *C3′H*, and this regimen was used in further experiments.

C3′H deficiency in *ref8* brings about severe growth defects and blocks the formation of sinapate esters as well as guaiacyl and syringyl lignin (Franke et al., 2002b; Li et al., 2010). Overall levels of lignin are also substantially reduced, and what is deposited is largely derived from *p*-hydroxyphenyl subunits. Without dex treatment, *ref8*^{pOpON} transgenic plants showed severe growth defects like *ref8* mutants, whereas growth retardation was greatly alleviated in *ref8*^{pOpON} plants exposed to a sustained dex treatment starting at seed imbibition (Fig. 2, A and B). Furthermore, the metabolic phenotype of *ref8*^{pOpON} was also substantially reverted by dex induction. HPLC analysis of extracts of uninduced *ref8*^{pOpON} rosette leaves confirmed the signature metabolic phenotypes of the *ref8* mutant, that is accumulation of *p*-coumarate esters, hyperaccumulation of flavonoids, and decrease of sinapate esters (Franke

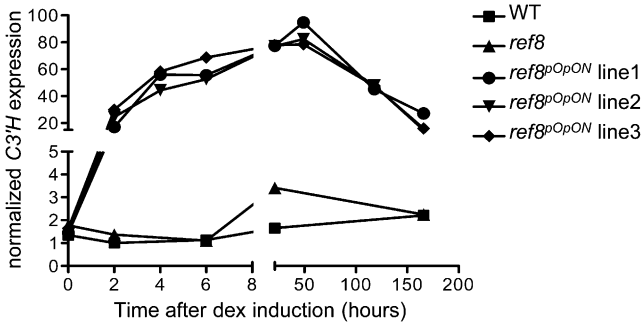

Figure 1. The induction of *C3′H* with dex in *ref8*^{pOpON} is rapid and stable. The relative expression levels of *C3′H* in wild-type (WT), *ref8*, and three *ref8*^{pOpON} lines were measured for 7 d after a single dex treatment. Two-week-old plants were sprayed with 20 μM of dex, and the whole rosette leaves were harvested at designated times after dex treatment for RNA extraction. The relative expression of *C3′H* was determined by quantitative RT-PCR using delta delta Ct method (Livak and Schmittgen, 2001). At1g13320 was used as an internal control.

et al., 2002a; Fig. 2, C–E). In the *ref8*^{pOpON} plants treated with dex, *p*-coumarate ester accumulation significantly decreased, and the content of flavonoids and sinapoylmalate was restored to wild-type levels. To examine if the lignin deposited in the *ref8* mutant was affected by induction of *C3′H*, we analyzed cell wall lignification by histochemical staining and the derivatization followed by reductive cleavage (DFRC) method (Lu and Ralph, 1997). The sections of uninduced *ref8*^{pOpON} stems stain poorly and aberrantly with both phloroglucinol-HCl and the Mäule reagent, consistent with a previous report showing that the two major types of lignin subunits in wild-type Arabidopsis, guaiacyl and syringyl units, are nearly eliminated in *ref8* mutants (Fig. 3A; Franke et al., 2002a). By contrast, *ref8*^{pOpON} plants treated with dex show staining and a lignification pattern similar to the wild type (Fig. 3A). Consistent with the histochemical staining results, lignin analysis using the DFRC method revealed that as in *ref8* plants (Franke et al., 2002a), *p*-hydroxylphenyl units, which are present in trace amounts in the wild type, are the major DFRC products in *ref8*^{pOpON} transgenic plants (Fig. 3B). By contrast, *ref8*^{pOpON} transgenic plants treated with dex accumulate significantly increased levels of guaiacyl and syringyl lignin compared with the untreated ones, but their *p*-hydroxylphenyl lignin content remains unchanged (Fig. 3B). These results indicate that dex application induced functional C3′H in stems and hypocotyls as well as in leaves of *ref8*^{pOpON} plants.

Induction of *C3′H* Expression in 3-Week-Old *ref8*^{pOpON} Plants Reveals Selective Turnover of Soluble Metabolite Pools in Leaves

To further study the changes in plant growth upon the induction of *C3′H* expression in *ref8*^{pOpON}, we monitored rosette leaf growth after applying dex to plants at 21 d after planting (DAP), a stage when wild-type Arabidopsis plants have rosette leaves of different ages, from newly emerging to fully expanded, but that have not yet bolted. We measured the fresh weight of individual leaf pairs at different time points after dex treatment. As shown in Figure 4, leaves of different ages showed different extents of growth restoration. Although young leaves of induced *ref8*^{pOpON} clearly grew bigger than that of uninduced plants, little dex-induced growth increase was observed for old leaves. Consistent with the observation for whole rosettes (Fig. 2B), despite significant relief of growth inhibition, the growth of young leaves of dex-induced *ref8*^{pOpON} plants was not restored to wild-type level (data not shown).

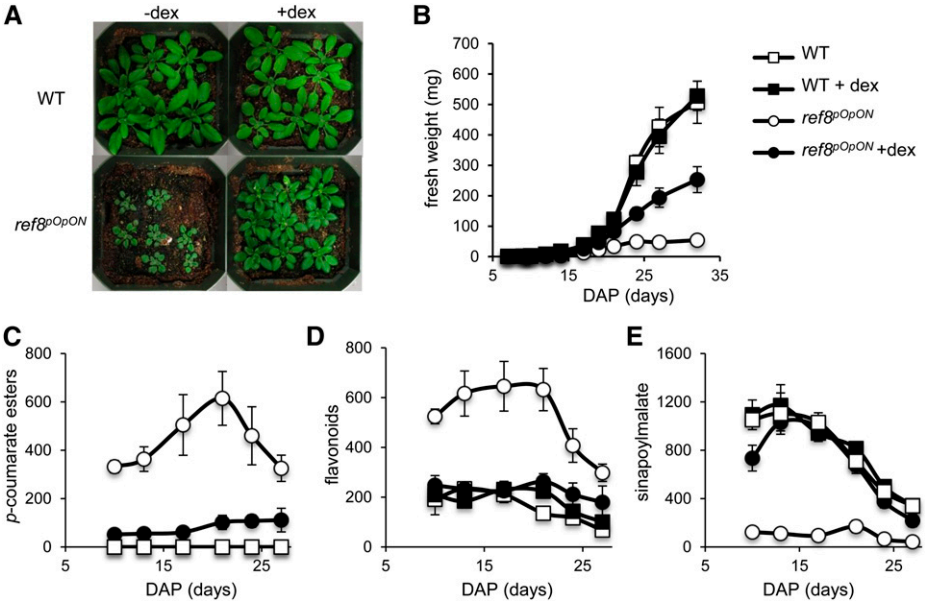

Figure 2. Dex-induced expression of *C3′H* substantially restores growth and soluble phenylpropanoid metabolite content of *ref8*^{pOpON}. Dex treatment was applied at the stage of seed imbibition and every 7 d thereafter. A, The wild type (WT) and *ref8*^{pOpON} grown with or without dex treatment were photographed at 24 DAP. B, Comparison of the fresh weight of the wild type and *ref8*^{pOpON} grown with or without dex treatment. C-E, The content of *p*-coumarate esters (the sum of *p*-coumaroylglucose, *p*-coumaroylshikimate, and *p*-coumaroylmalate levels; C), flavonoids (the sum of kaempferol 3-*O*-[6′′-*O*-(rhamnosyl) glucoside] 7-*O*-rhamnoside, kaempferol 3-*O*-glucoside 7-*O*-rhamnoside, and kaempferol 3-*O*-rhamnoside 7-*O*-rhamnoside levels; D), and sinapoylmalate (E) of wild-type and *ref8*^{pOpON} plants with or without dex treatment. Data for the wild type and the wild type plus dex overlap in C. Wild-type plants do not accumulate *p*-coumaroyl esters regardless of dex application. The ordinate units of graphs C to E are pmol mg^{-1} fresh weight. All graphs show the average of three biological replicates, and the error bars represent SD. [See online article for color version of this figure.]

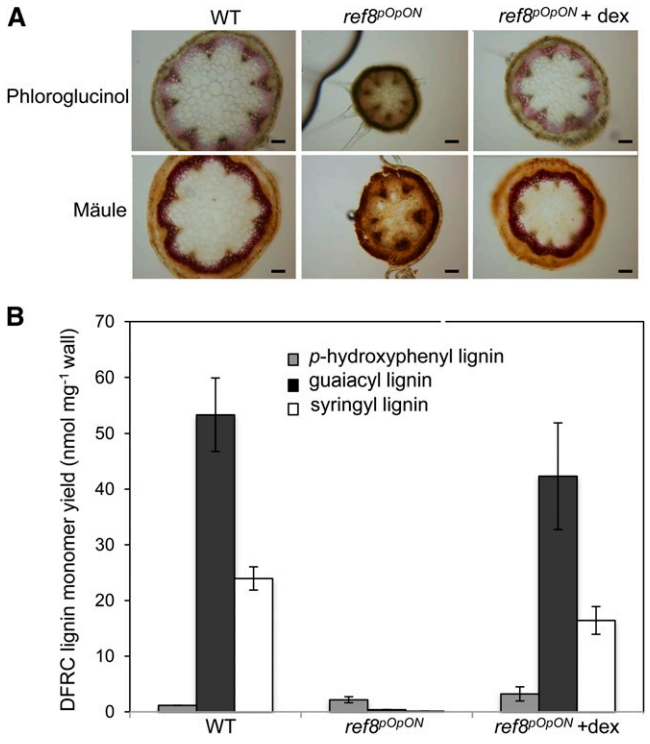

Figure 3. Dex-induced expression of *C3′H* restores lignification of *ref8*^{pOpON}. A, Histochemical staining of primary inflorescence stems of wild type (WT), *ref8*^{pOpON} without dex treatment (*ref8*^{pOpON}), and *ref8*^{pOpON} with dex treatment (*ref8*^{pOpON} + dex). Stems from 2-month-old plants were sectioned using a vibratome and stained with phloroglucinol and Mäule staining solution. Dex treatment was applied at the stage of seed imbibition and every 7 d thereafter. At least three plants for each treatment were analyzed, and similar results were observed. Bars = 100 μm. B, DFRC lignin contents of wild-type and *ref8*^{pOpON} plant with or without dex treatment. Average values of three biological replicates were shown, and the error bars represent SD.

It was previously shown that *p*-coumarate esters and flavonoids are hyperaccumulated in *ref8* mutants, whereas the content of sinapate esters such as sinapoylmalate is decreased (Franke et al., 2002a, 2002b; Weng et al., 2010). To investigate the impact of C3′H induction on these soluble phenylpropanoid metabolites in *ref8*^{pOpON}, we measured the temporal changes of *p*-coumarate ester, flavonoid, and sinapoylmalate content in individual leaves, in parallel with the growth measurements described above. Similar to the way induction impacts growth of young leaves more than old leaves, flavonoid and sinapoylmalate accumulation is more sensitive to the induction of *C3′H* expression in young leaves than in older ones (Fig. 5, A and B). Although a decrease in flavonoids and an increase in sinapoylmalate levels were clearly observed in young and newly emerging leaves within 3 d after dex application, the oldest leaves still contained relatively unchanged levels of these compounds even 6 d after dex application. As shown in Figure 5C, *p*-coumarate esters were accumulated in all rosette leaves of *ref8*^{pOpON} plants but were near to or below the limits of detection in the wild type. In contrast to the results observed with flavonoids and sinapoylmalate, when dex was applied to *ref8*^{pOpON}, the content of *p*-coumarate esters in all rosette leaves dropped significantly after 3 d and reached wild-type levels within 6 d. Taken together, these results indicates that in old leaves, selective turnover of leaf soluble phenylpropanoid metabolites occurs in C3′H-induced *ref8*^{pOpON} plants.

Activation of C3′H at Different Developmental Stages Has Distinct Impacts on Plant Growth

To determine whether the timing of *C3′H* expression induction determines the extent to which the *ref8* dwarf phenotype can be alleviated, we attempted to rescue *ref8*^{pOpON} plants by starting dex treatments at different developmental stages (Fig. 6). Compared with the uninduced control, all the *ref8*^{pOpON} plants that received an initial dex application between 0 and 49 DAP showed substantial alleviation of dwarfism and restoration of fertility; however, there was a clear distinction of the growth phenotype between the *ref8*^{pOpON} plants that were induced before 28 DAP and those induced at later stages of growth (Fig. 6A). Growth of the primary inflorescence stem was restored to a similar extent among the *ref8*^{pOpON} plants with a dex treatment starting before 28 DAP, a time that coincided with bolting under our growth condition (Fig. 6B). By contrast, dex induction starting at later times promoted generation of secondary rosette inflorescences from axillary meristems but did not relieve much of the growth inhibition of their primary shoots (Fig. 6B).

It has often been assumed that deficiency in lignification of tracheary elements and concomitant failure of normal water transport are responsible for the dwarfism exhibited by lignin mutants such as *ref8*. To examine the association between lignification, vascular structure, and the growth restoration of dex-treated *ref8*^{pOpON} plants, we performed phloroglucinol-HCl and Mäule staining on cross sections of primary shoots and hypocotyls. As shown in Figure 3A, whereas clear staining similar to what was observed in the wild type was seen in both stems and hypocotyls of 0 DAP-induced *ref8*^{pOpON} plants with either phloroglucinol-HCl or Mäule reagent, poor lignification in the untreated plants was evident from very weak staining with either reagent. The *ref8*^{pOpON} plants induced between 0 and 28 DAP showed a staining pattern in their primary inflorescence stems similar to the wild type, but the plants induced at later stages showed much weaker staining (Fig. 6C). These results parallel the observation that plants treated earlier with dex showed much greater restoration of primary inflorescence growth than the plants induced after 28 DAP (Fig. 6B). The 35 DAP-induced *ref8*^{pOpON} plants gave a positive but weak reaction with phloroglucinol-HCl and Mäule reagent, although variation was seen between shoot and hypocotyl staining. By contrast, changes in the staining of 42 DAP-induced plants were nearly undetectable (Fig. 6C).

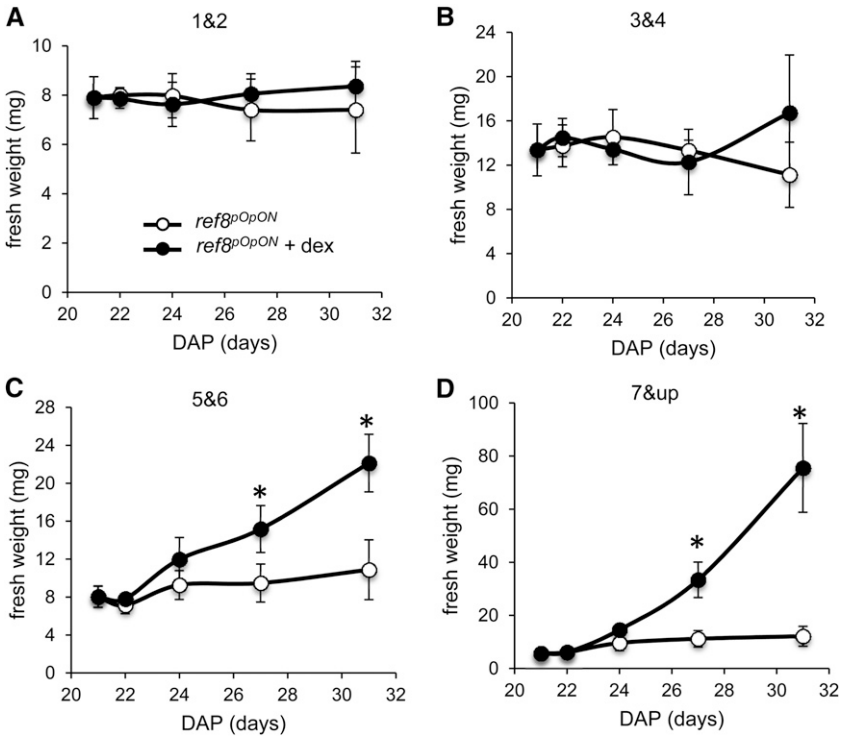

Figure 4. Induction of *C3′H* expression in 3-week-old *ref8*^{pOpON} plants is more effective at restoring growth in young leaves compared with more mature leaves. A to D, Fresh weight of individual leaf groups. The oldest rosette leaf was counted as the first leaf. The total fresh weight of first and second leaves (1&2, A), third and fourth leaves (3&4, B), fifth and sixth leaves (5&6, C), and seventh and any newly emerging leaves (7&up, D) are shown. White circles represent *ref8*^{pOpON} without dex treatment, and black circles represent *ref8*^{pOpON} with dex treatment. Data shown are the average of four biological replicates, and the error bars represent SD. Student's *t* test was performed to compare the leaf weight between dex-treated and untreated *ref8*^{pOpON} plants for each time point, and a *P* value less than 0.05 was indicated by an asterisk.

Although the primary stems of 35 and 42 DAP-induced *ref8*^{pOpON} plants were not strongly stained, the newly emerged rosette inflorescence stems of those plants stained like the wild type (Fig. 6D). The *ref8*^{pOpON} plants induced at 49 DAP produced new shoots within 1 week of induction (Fig. 6A, insert), but their primary inflorescence stems and hypocotyls showed little phloroglucinol-HCl and Mäule staining, similar to untreated *ref8*^{pOpON} plants (Fig. 6C).

Thin sections of hypocotyls of the 56-DAP wild-type and *ref8*^{pOpON} plants that received different dex treatment at different times were examined by confocal scanning laser microscopy to investigate at higher magnification the structural changes of the vascular tissue that resulted from *C3′H* induction. The untreated *ref8*^{pOpON} has poorly formed secondary cell walls in the secondary xylem and vascular cambium (Fig. 7, C and D) compared with the wild type (Fig. 7, A and B). However, the 0 DAP-induced plants have few (essentially one ring) similarly malformed cells, but the majority appears structurally competent (Fig. 7, E and F), similar to the wild type. The majority of the vascular cells of the 49 DAP-induced *ref8*^{pOpON} look similar to those of the untreated plants but appear to have one newly formed secondary xylem layer (adjacent to the vascular cambium) with properly formed cell walls (Fig. 7, E and G). These data are consistent with the hypothesis that the expression of *C3′H* in the *ref8* mutants relieves the growth inhibition by permitting the deposition of normal xylem to restore water transport, although we cannot exclude the possibility that, alternatively or additionally, other changes to phenylpropanoid metabolism may be important in the growth restoration.

Reduction of SA Content Does Not Rescue Dwarfism in *ref8* Mutants

Given the recent report that SA accumulation is responsible for the dwarf phenotype of some phenylpropanoid mutants (Gallego-Giraldo et al., 2011), we measured SA levels in *ref8*^{pOpON} plants before and after treatment with dex. SA content in *ref8*^{pOpON} plants was about 2-fold higher than in the wild type and dropped to the wild-type level following dex treatment (Fig. 8).

To test if the increased SA levels caused the growth inhibition in *ref8* mutants, we crossed *ref8*^{pOpON} with a *NahG*-expressing transgenic line. *NahG* encodes a bacterial salicylate hydroxylase that converts SA to catechol, and it has been shown that plants overexpressing *NahG* contain reduced levels of SA (Delaney et al., 1994; Lee et al., 2007). From the population of 142 individual F2 plants generated, we randomly selected three wild-type plants, eight plants that were *REF8* homozygous and carry *NahG* but not the *pOpON*:*C3′H* transgene, two *ref8* homozygous plants that did not carry either transgene, and 10 plants that were homozygous for *ref8* and carried the *NahG* but not the *pOpON*:*C3′H* transgene. We then compared the leaf fresh weight and plant height of the F2 plants from these four genotypes. It is clear that although the *NahG* transgene reduced the SA accumulation, it had no impact on the growth phenotype of *ref8*

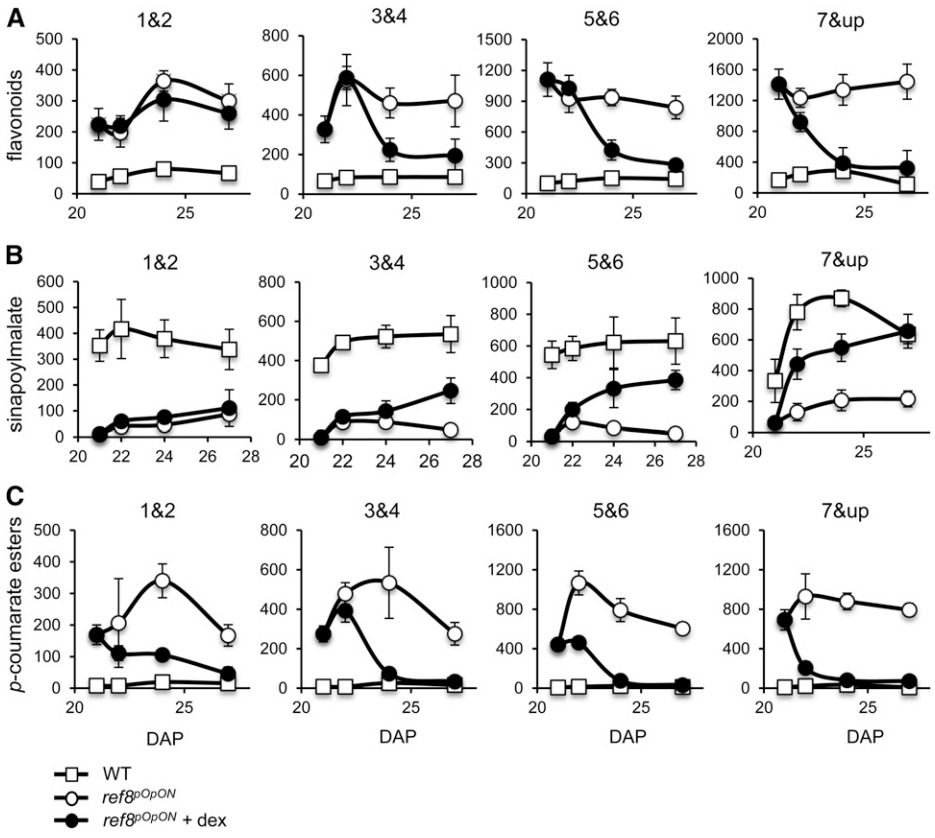

Figure 5. Comparison of temporal changes of soluble phenylpropanoid metabolite content in leaves of different ages between the wild type (WT), *ref8*^{pOpON} without dex treatment (*ref8*^{pOpON}), and *ref8*^{pOpON} treated with dex at 21 DAP (*ref8*^{pOpON} + dex). A to C, The content of flavonoids (the sum of kaempferol 3-*O*-[6′′-*O*-(rhamnosyl) glucoside] 7-*O*-rhamnoside, kaempferol 3-*O*-glucoside 7-*O*-rhamnoside, and kaempferol 3-*O*-rhamnoside 7-*O*-rhamnoside; A), sinapoylmalate (B), and *p*-coumarate esters (the sum of *p*-coumaroylglucose, *p*-coumaroylshikimate, and *p*-coumaroylmalate; C) in first and second leaves (1&2), third and fourth leaves (3&4), fifth and sixth leaves (5&6), and seventh and any newly emerging leaves (7&up). The unit for the ordinate of all graphs is pmol mg^{-1} fresh weight. White squares represent the wild type, white circles represent *ref8*^{pOpON} without dex treatment, and black circles represent *ref8*^{pOpON} with dex treatment. Data shown are the average of four biological replicates, and the error bars represent SD.

plants (Figs. 8 and 9). These results suggest that the hyperaccumulation of SA is unlikely to be responsible for the dwarfism of *ref8* mutants.

DISCUSSION

Perturbation of phenylpropanoid metabolism often results in growth and developmental defects such as dwarfism and sterility. Lignin is a major product of the phenylpropanoid pathway, with important biological functions as a component of the cell wall that confers mechanical strength and hydrophobicity to tracheary elements. As a result, it has been suggested that the dwarf phenotype of phenylpropanoid-defective mutants may be attributable to vascular collapse due to lignin deficiency and the ensuing impact of these architectural changes on water transport. A recent physiological study of C3′H-down-regulated poplar trees revealed that the xylem of these plants exhibits decreased hydraulic conductivity and is more prone to cavitation (Coleman et al., 2008). However, although collapsed xylem has been observed for lignin-compromised plants in various species (Elkind et al., 1990; Jones et al., 2001; Piquemal et al., 1998; Reddy et al., 2005; Coleman et al., 2008; Schilmiller et al., 2009), it is not clear if this is the primary cause of the growth reduction phenotype or a coincident effect.

It is noteworthy that growth inhibition occurs very early in some Arabidopsis phenylpropanoid mutants such as *ref3* and *ref8*, and in the most severe cases, the plants do not produce inflorescence stems at all. In Arabidopsis, the first sign of lignification can be observed in the radicle and cotyledons of seedlings as early as 48 h postimbibition (Dharmawardhana et al., 1992). Nevertheless, it seems that de novo lignin biosynthesis is not essential for germination or cotyledon development because the null mutants of *C4H* germinate and develop cotyledons (Schilmiller et al., 2009; J.I. Kim and C. Chapple, unpublished data). By exploiting a dex-inducible gene expression system (Craft et al., 2005), we were able to activate the expression of an Arabidopsis *C3′H* transgene in the *ref8* mutant with precise temporal control. This allowed us to examine the dynamic changes in lignification, growth restoration, and soluble phenylpropanoid accumulation upon restoration of C3′H function.

The *ref8* mutant exhibits several characteristic changes in its soluble phenylpropanoid metabolite profile compared with the wild type. The metabolic blockage at C3′H directly results in reduced production of sinapoylmalate and the accumulation of *p*-coumarate esters such as *p*-coumaroyl shikimate, *p*-coumaroylmalate, and *p*-coumaroylglucose (Franke et al., 2002a). In addition, the levels of flavonoids are significantly increased, either because that restriction of the lignin biosynthetic pathway leads to the channeling of metabolic flux to the interconnecting flavonoid branch (Besseau et al., 2007) or because the metabolic block in

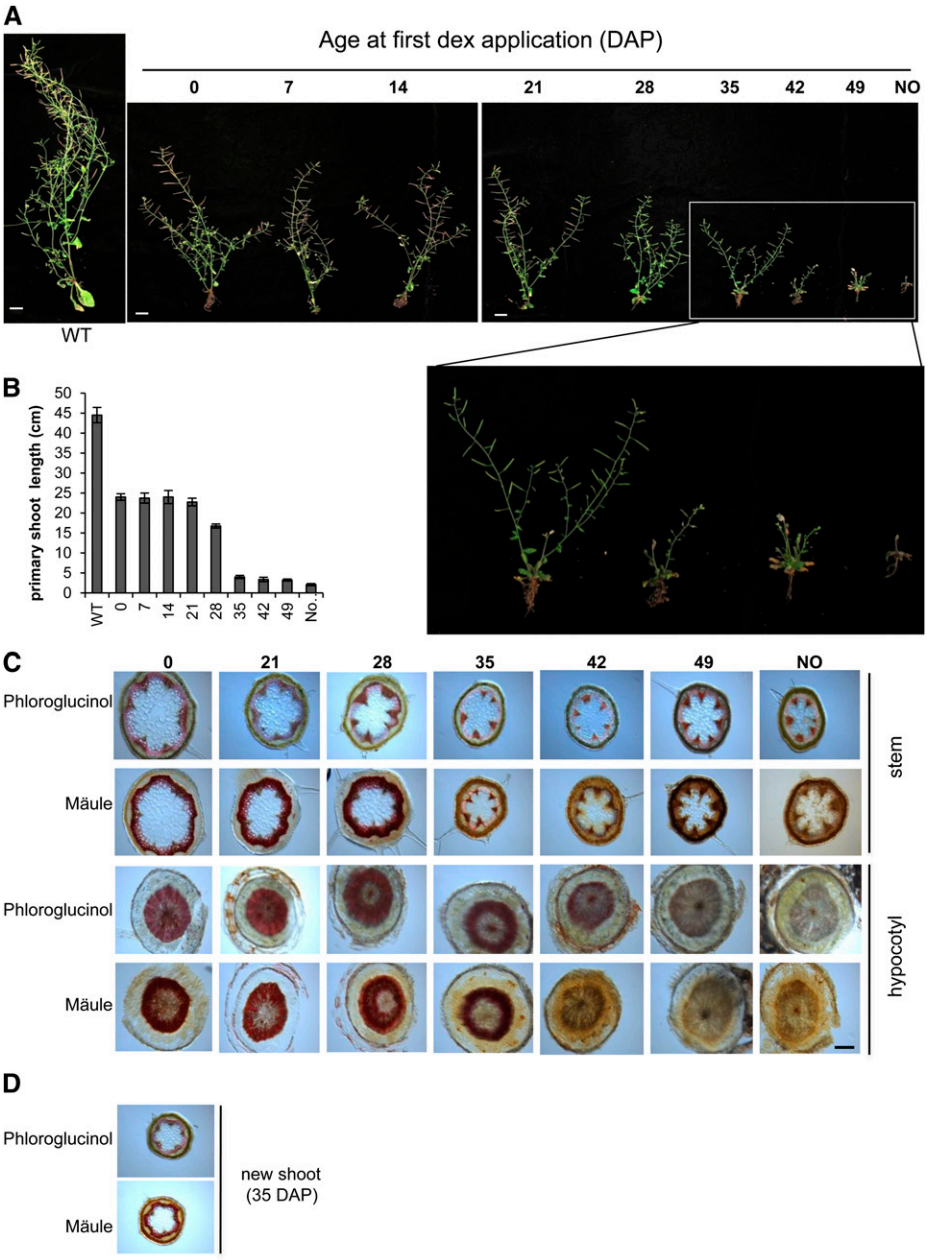

Figure 6. Induction of *C3′H* expression in mature *ref8*^{pOpON} enables the plants to make new shoots without changing lignification of the hypocotyl and primary inflorescence stem. A, Fifty-six-day-old *ref8*^{pOpON} plants with dex treatment at various time points are shown and compared with the wild type (WT). The numbers indicate DAP when the first dex treatment occurred. Dex was sprayed every 7 d after the first application. Bars = 2 cm. B, The primary shoot length of the plants shown in A. C, Phloroglucinol-HCl and Mäule staining of primary inflorescence stems (top two rows) and hypocotyls (bottom two rows) of 56-d-old *ref8*^{pOpON} plants. The number indicates the DAP when the first dex application occurred. D, Phloroglucinol-HCl and Mäule staining of the newly emerged inflorescence stem on 56-d-old *ref8*^{pOpON} plants that received dex treatments starting at 35 DAP. NO, No dex treatment.

the mutant initiates a stress signaling pathway that results in flavonoid hyperaccumulation (Dixon and Paiva, 1995; Fini et al., 2011). Our data show that induced *C3′H* expression in *ref8* has different effects on the accumulation of these metabolites depending upon the tissue being examined. Restoration of functional C3′H in *ref8*^{pOpON} plants has little effect on flavonoid accumulation in mature leaves, in contrast to the rapid decrease of *p*-coumarate esters observed in both young and old leaves. This suggests that vacuolar secondary metabolites are turned over upon dex induction in the *ref8*^{pOpON} system and that these processes may occur in the wild type as well. Metabolic turnover of phenylpropanoid metabolites is largely an unexplored area. Our current knowledge is limited to the turnover of coniferin in pine (*Pinus* spp.) and salicylates in willow (*Salix* spp.) from a few early studies (Marcinowski and Grisebach, 1977; Ruuhola and Julkunen-Tiitto, 2000). The inducible *ref8*^{pOpON} plant we have generated during this study provides a good opportunity for further investigating the turnover of different phenylpropanoid metabolites.

Depletion of *p*-coumarate esters in *ref8*^{pOpON} plants after dex treatment suggests that upon C3′H activation, these compounds may reenter the previously blocked phenylpropanoid pathway and contribute to the synthesis of lignin and sinapoylmalate. Considering that the *p*-coumarate esters are located in vacuole (Strack

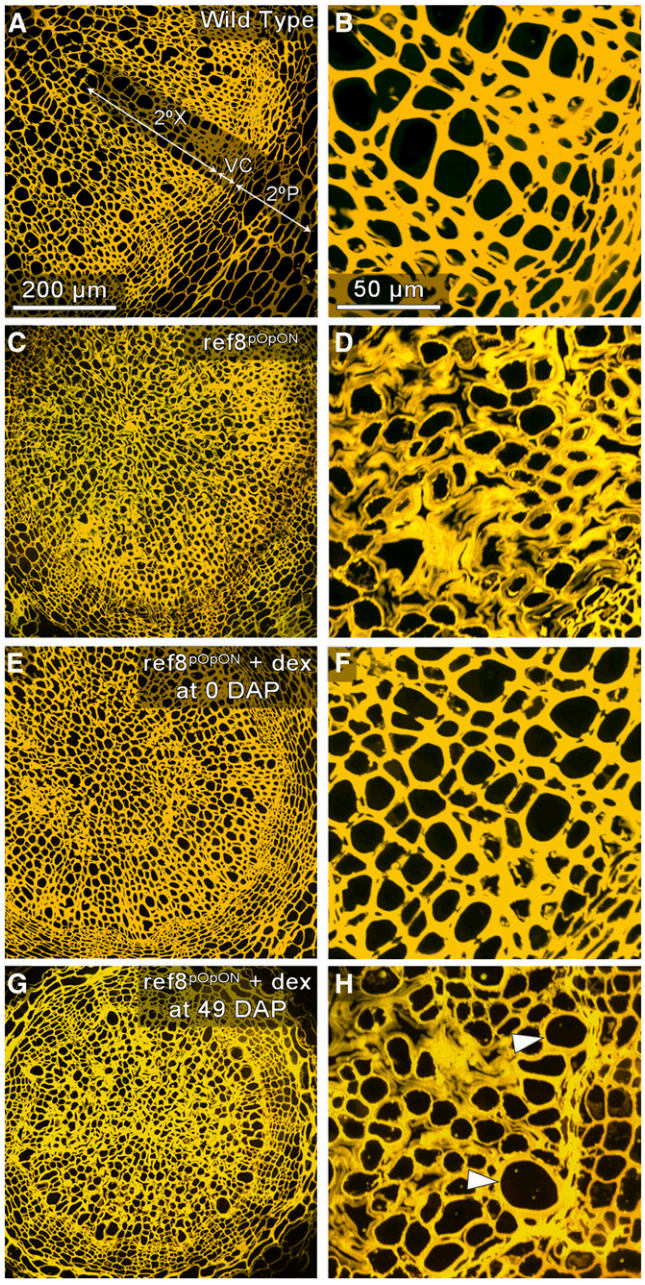

Figure 7. Confocal scanning laser microscopy of 56-d-old hypocotyls. A and B, Wild-type hypocotyl showing structurally competent vascular cell walls. 2°X, Secondary xylem; 2°P, secondary phloem; VC, vascular cambium. C and D, Vascular tissue of the *ref8* mutant contains predominantly malformed cell walls with occluded lumen in many locations. E and F, Hypocotyls from the *ref8*^{pOpON} plants treated with dex 0 DAP exhibit mainly structurally competent vascular cell walls similar to the wild type. G and H, Hypocotyls from the *ref8*^{pOpON} plants treated with dex 49 d after germination have mostly malformed cell walls in the vascular tissue but contain approximately one layer of structurally competent secondary xylem cells adjacent to the vascular cambium (indicated by arrowheads in H). Images in each column are identical in scale. [See online article for color version of this figure.]

and Sharma, 1985) and C3′H is in the cytoplasm, this would require these compounds to be exported from the vacuole. Alternatively, the preaccumulated *p*-coumarate esters may be degraded through some unknown catabolic pathway, and the rise in sinapoylmalate levels observed in our experiments may be due to de novo synthesis. The fact that the onset of *C3′H* expression restores sinapoylmalate to wild-type levels more effectively in young leaves than in older ones may be attributed to the differences in sinapate ester biosynthetic capacity between the leaves at different stages. For example, it is known that sinapoylmalate accumulation in Arabidopsis is developmentally regulated and the transcript of *ferulate5-hydroxylase* (*F5H*), a gene required for sinapate ester biosynthesis, is abundant in young leaves but barely detectable in mature leaves (Ruegger et al., 1999). Thus, F5H deficiency may still limit sinapate ester production in old leaves of dex-induced *ref8*^{pOpON} plants even when the metabolic blockage at C3′H is overcome.

Similar to what has been observed for the *ref8* biochemical phenotypes, our data show that induction of *C3′H* expression in *ref8*^{pOpON} generally is more effective in rescuing growth in young leaves than in old ones. Leaf growth involves a set of successive developmental events including cell proliferation and cell expansion. Kinematic analysis of leaf growth in Arabidopsis revealed that leaf size increases exponentially at early

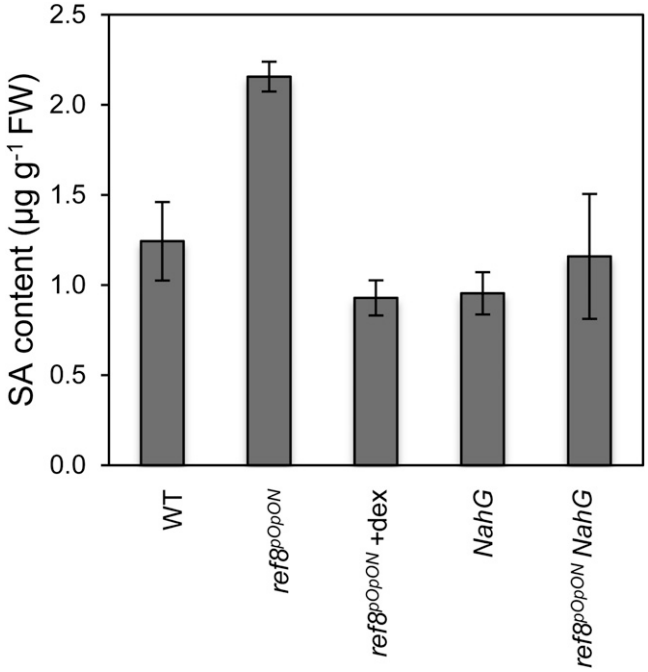

Figure 8. Comparison of SA content in the wild type and plants with different genotypes or treatments. SA content in whole rosette from 4-week-old plants was measured using a liquid chromatography-mass spectrometry-based method. Dex treatment was applied starting at 0 DAP. Data shown are the average of three biological replicates, and the error bars represent SD.

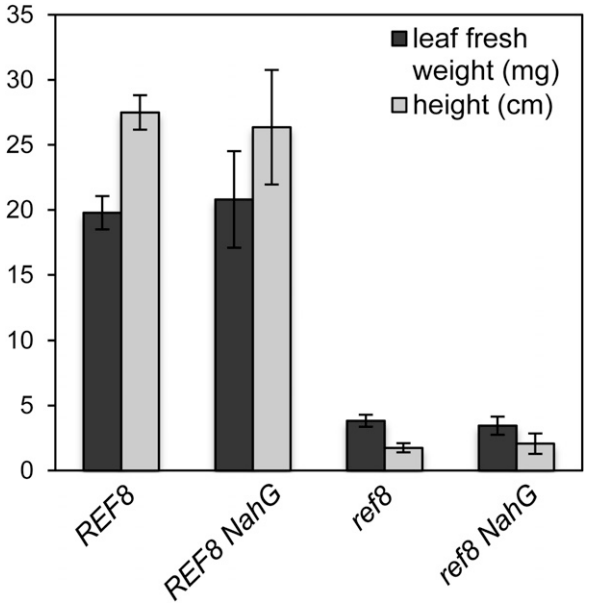

Figure 9. Reduction of SA by *NahG* expression does not alleviate growth defects in the *ref8* mutant. A cross between *ref8*^{pOpON} and a *NahG*-expressing transgenic line was made, and different genotypes of F2 plants were selected and measured for leaf fresh weight and plant height. *REF8* indicates plants homozygous for *C3′H*; *REF8 NahG* indicates plants homozygous for *C3′H* and carrying the *NahG* transgene; *ref8* indicates plants homozygous for *ref8*; and *ref8 NahG* indicates plants homozygous for *ref8* and carrying the *NahG* transgene. The average of the fresh weight of the third and fourth rosette leaves on 3-week-old plants was used for this analysis. Plant height was measured by the length of primary inflorescence stem when the plants are 5 weeks old. Data represent mean ± SD ($n = 3$ for *REF8*; $n = 2$ for *ref8*; $n = 8$ for *REF8 NahG*; $n = 10$ for *ref8 NahG*).

stages, and later, the growth rate gradually slows down until the leaf reaches its final size (Beemster et al., 2005; Mündermann et al., 2005). Our observation that *C3′H* expression in *ref8* leads to increased expansion of young leaves but not old leaves suggests that although C3′H deficiency limits leaf size increases, it does not prevent the leaf from proceeding through different developmental stages. Therefore, despite their reduced size, the old leaves of *ref8* may have already reached maturity, so they cannot grow any larger, whereas younger leaves still have the competency to expand when C3′H deficiency is alleviated.

In our experiments, even with a dex treatment starting at the seed imbibition stage, *ref8*^{pOpON} plants do not grow as tall as the wild type, and their hypocotyl vasculature still has at least one layer of collapsed xylem tissue. Given that a dex-inducible construct has been successfully used to overexpress a G-protein gene in Arabidopsis during seed germination (Ullah et al., 2002), it seems that lack of *C3′H* during early seedling development is unlikely to be the cause of the incomplete rescue we have observed. One possible explanation for this result is that the levels of *C3′H* expression we measure may not be representative of the expression levels in cells where *C3′H* is normally expressed. Because the inducible promoter used in this study is controlled by a 35S-driven transcription factor, it is likely that in the induced *ref8*^{pOpON} plants, *C3′H* is expressed in cells where *C3′H* is normally not expressed in wild-type Arabidopsis. This means that our quantitative RT-PCR results overestimate the level of *C3′H* mRNA where its expression is relevant, and in those relevant cells, *C3′H* expression may be insufficient to fully complement the *ref8* mutant phenotype. For example, it is known that the 35S promoter does not target gene expression strongly to the cells where phenylpropanoid metabolism normally occurs, as evidenced by the fact that overexpression of *F5H* using a 35S promoter is much less effective in increasing syringyl lignin levels compared with using the promoter of *C4H* gene (Meyer et al., 1998; Franke et al., 2000).

Interestingly, switching on *C3′H* expression at different time points before bolting restored the growth of primary inflorescence stems in *ref8*^{pOpON} plants to a similar extent. By contrast, the *ref8*^{pOpON} plants induced near to or after bolting showed a much more limited alleviation of the growth inhibition of their primary inflorescence stems than those induced at earlier times. Because the bolting transition is an important indicator of reproductive phase change in Arabidopsis, during which dramatic alteration in plant body form and shoot meristems occur (Poethig, 2003; Pouteau and Albertini, 2009), it is tempting to speculate that phenylpropanoid metabolism may play an important role in determining the growth potential of the primary inflorescence stem at a developmental stage immediately preceding or during the transition from a vegetative to a reproductive state. Alternatively, the efficacy of *C3′H* expression in growth restoration may be limited by the increased cross linking of cell wall components and secondary wall thickening during inflorescence stem development (Altamura et al., 2001; Cosgrove, 2005). Although *C3′H* expression seems to have little effect on stems after bolting, it provides permissive conditions for the production of new inflorescence stems from the rosette.

Collapsed xylem and dwarfism are often observed in mutants defective in various components of the secondary cell wall including lignin, cellulose, and xylan (Turner and Somerville, 1997; Jones et al., 2001; Brown et al., 2005; Persson et al., 2007). This association suggests that the growth of these mutants is limited by water transport deficiency resulting from these xylem abnormalities. The dwarf phenotype of *ref3* and the three Arabidopsis xylan mutants *irregular xylem7* (*irx7*), *irx8*, *and irx9* can be effectively alleviated by expressing the cognate wild-type genes specifically in the water-transducing vessels of these mutants (Petersen et al., 2012; Yang et al., 2013). Whereas only end point phenotypic changes could be observed in these previous studies, the chemical induction system used in this work allowed us to turn on the lignin biosynthetic pathway at a certain time point and follow the early biochemical and structural changes of vasculature as

related to the plant growth response. The relief of growth arrest of *ref8* is tightly linked to the appearance of normal xylem vessels, and it is striking that a single layer of normal vessel elements in the hypocotyl seems to be sufficient to support the initiation and growth of new rosette inflorescence stems.

In addition to compromised water transport, there is also evidence for impaired homeostasis or perception of plant hormones in the dwarfism of phenylpropanoid mutants. The growth inhibition observed in HCT-suppressed Arabidopsis has been attributed to reduced auxin polar transport (Besseau et al., 2007), although it is not clear how this hormone effect might be brought about by the defect of phenylpropanoid metabolism in those plants (Li et al., 2010). Arabidopsis mutants that accumulate high levels of SA also display dwarf phenotypes (Bowling et al., 1994; Petersen et al., 2000; Li et al., 2001; Lee et al., 2007). A recent study reported that Arabidopsis HCT RNAi plants contain elevated SA levels and the dwarfism of these plants can be alleviated by reducing the levels of SA by genetically blocking its formation or enhancing its degradation (Gallego-Giraldo et al., 2011). Considering the close positioning of HCT and C3′H in the phenylpropanoid pathway, we anticipated that the same would be true for *ref8* mutants. The *ref8* mutant does contain higher levels of SA compared with the wild type; however, reducing the content of SA in *ref8* by overexpressing the *NahG* transgene does not rescue the dwarf phenotype. Thus, it seems unlikely that the dwarfism of Arabidopsis *ref8* mutants depends on SA accumulation, suggesting the presence of multiple underlying mechanisms for the growth defects of lignin-deficient mutants. However, we cannot exclude the possibility that the 35S-driven *NahG* overexpression in *ref8* may not be effective in reducing SA accumulation in certain cell types or tissues that affects plant growth. Further spatial and temporal controlled experiments on SA accumulation and plant growth in the *ref8* mutant may be useful to better understand the underlying mechanism for its dwarfism.

MATERIALS AND METHODS

Plant Material and Growth Conditions

Arabidopsis (*Arabidopsis thaliana*) plants grown in soil were cultivated at a light intensity of 100 μE m^{-2} sec^{-1} at 21°C under a photoperiod of 16-h light/8-h dark in a growth chamber. Ecotype Columbia was used as the wild type; the *ref8* mutant has been described previously (Franke et al., 2002b).

Generating *ref8*^{pOpON}-Inducible Lines

To generate *pOpON*:*C3′H*-inducible construct, the Arabidopsis *C3′H* genomic region was amplified by PCR using the primer pair 5′-GGGGACAAGTTTGTACAAAAAAGCAGGCTCAAAACTTCATGTCGTGGTTTC-3′ and 5′-GGGGACCACTTTGTACAAGAAAGCTGGGTAACTTGTTCTTATGTCCTGCAAAT-3′. The PCR product was cloned into a Gateway entry vector that was modified from pENTR1A (Life Technologies, http://www.lifetechnologies.com) by replacing the kanamycin selection marker with an ampicillin resistance gene. The resulting *C3′H* entry clone was recombined with *pOpON* (Craft et al., 2005) to generate the *pOpON*:*C3′H* construct, which was introduced into *ref8* heterozygous plants via *Agrobacterium tumefaciens*-mediated transformation. T1 seeds were planted on Murashige and Skoog media containing 50 μg mL^{-1} kanamycin, and the resistant seedlings were transferred to soil after 1 week. Dwarf T1 plants were kept and sprayed with dex to obtain T2 seeds. The homozygosity of *ref8* in those lines was evaluated by performing PCR using the primer pair CC2831 and CC2832, 5′-CGAGCTATCATGGAGGAGCATA-3′ and 5′-CAACAAGAGCATGAGCAGCAG-3′ in combination with *Eco*RV digestion as described previously (Franke et al., 2002b). Copy number of the transfer DNA insertion was evaluated by segregation of the kanamycin resistance phenotype in individual T3 lines.

Plant Growth Measurement and C3′H Induction

To induce *C3′H* early in plant development, *ref8*^{pOpON} seeds were soaked in a solution containing 20 μM dex for 4 d (0 DAP). Alternatively, *ref8*^{pOpON} plants were grown without dex and were then sprayed with a solution containing 20 μM dex at various times after planting and then every 7 d thereafter. For secondary metabolite analyses, whole rosette or individual leaves were detached, weighed, and stored in liquid nitrogen. For leaf metabolite analysis, the first and second leaves were combined as one sample, so were the third and fourth or the fifth and sixth leaves. The seventh and any younger leaves were combined together as a single sample.

Quantitative RT-PCR

Total RNA was isolated from Arabidopsis rosette leaves using the RNeasy Plant Mini Kit (Qiagen, http://www.qiagen.com). Each RNA sample was treated with TURBO DNase (Life Technologies, http://www.lifetechnologies.com) at 37°C for 1 h to eliminate DNA contamination. One microgram of RNA was used for complementary DNA (cDNA) synthesis. cDNA was synthesized with a high-capacity cDNA RT kit (Life Technologies) following the protocol provided by the manufacturer. Quantitative RT-PCR was performed using Fast SYBR Green Master Mix (Life Technologies). *C3′H* was amplified using the primer pair CC2839 and CC2840, 5′-CAAAGGATCAAACGTTCATGTGA-3′ and 5′-TTCCATACAGCCGGGTCTCT-3′.

At1g13320 was used as an internal control, and the primer pair CC2558 and CC2559, 5′-TAACGTGGCCAAAATGATGC-3′ and 5′-GTTCTCCACACCGCTTGGT-3′ was used for the amplification (Czechowski et al., 2005). Relative expression of *C3′H* was calculated using the delta delta Ct method (Livak and Schmittgen, 2001).

HPLC Analysis of Soluble Metabolites

Rosette leaves were harvested and stored in liquid nitrogen for extraction of soluble metabolites. Frozen tissues were extracted with 50% (v/v) methanol at 65°C for 40 min. Samples were centrifuged at 16,000*g* for 5 min before loading on HPLC. Ten microliters of extract was separated on a Shim-pack XR-ODS column (3.0 × 75 mm, 2.2 μm; Shimadzu, http://www.shimadzu.com) using 0.1% (v/v) formic acid in water as solvent A and acetonitrile as solvent B at a flow rate of 1 mL min^{-1} with the method used previously (Li et al., 2010). Sinapic acid, *p*-coumaric acid, and kaempferol were used as standards for quantification of sinapoylmalate, *p*-coumarate esters, and flavonoids, respectively.

Lignin Analysis

For lignin monomer analysis, 56-d-old plant stem samples were harvested, ground in liquid nitrogen, and extracted once with 0.1 mM sodium phosphate buffer (pH 7.2) at 50°C and 70% (v/v) ethanol at 70°C six times. DFRC lignin analysis was performed as previously reported (Weng et al., 2010).

Histochemical Staining

The base of primary inflorescence stems or hypocotyls were embedded in 5% agar and were cut into 100-μm sections using a vibratome. Phloroglucinol-HCl staining and Mäule staining were performed as previously described with slight modification (Chapple et al., 1992). For phloroglucinol-HCl staining, the staining solution was made with 16% (v/v) ethanol, 10% (v/v) HCl, and 20 mg mL^{-1} phloroglucinol. Plant sections were incubated in 0.2% phloroglucinol solution for 10 min and mounted in water. For Mäule staining, sections were incubated in 0.5% potassium permanganate solution for 10 min and

rinsed with water twice, 10% (w/v) HCl for 5 min and rinsed with water twice, and mounted in concentrated ammonium hydroxide.

Confocal Scanning Laser Microscopy

Hypocotyl tissue immediately below the rosette was fixed in 2% (v/v) glutaraldehyde and processed by microwave embedding. The samples were dehydrated by treating with increasing concentrations of acetone in a Pelco laboratory microwave oven (Ted Pella) for 1 min for each dilution (15% [v/v], 30% [v/v], 60% [v/v], 90% [v/v], and three times with 100% [v/v] acetone). After dehydration, the samples were infiltrated with Eponate 812 (EMS) by incubating at room temperature for several hours to overnight in increasing concentrations of resin (15% [v/v], 30% [v/v], 60% [v/v], 90% [v/v], and three times with 100% [v/v] resin, diluted in acetone). The samples were transferred to capsules, and the resin was polymerized in an oven at 60°C overnight. Semithin (250-nm) sections were positioned on glass microscope slides and stained with 0.2% (w/w) acriflavine for confocal scanning laser microscopy of cell walls. Images were captured using a Nikon C1 Plus confocal microscope operated via Nikon's EZ-C1 software using a 488-nm excitation laser.

Analysis of *NahG ref8* Plants

Crosses were made between *ref8*^{pOpON} plants and *NahG* overexpression plants (Delaney et al., 1994). F2 seeds were planted on soil without dex treatment. One hundred forty-two 3-week-old individual F2 plants were analyzed for their genotypes and growth phenotypes. Genomic DNA was prepared with Phire Plant Direct PCR Kit (Finnzymes, http://www.thermoscientificbio.com/finnzymes) following the protocol provided by the manufacturer. The *ref8* mutation was confirmed using the method described above. The *pOpON:C3′H* transgene was detected by performing PCR using the primer pair CC2831 and CC1897, 5′-AATGCGTGGTGAAAGAGTCA-3′ and 5′-TGCAGGAGTTCAAGGAATCA-3′. The presence of the *NahG* transgene was evaluated by performing PCR with the primer pair CC3887 and CC3888, 5′-ACTGGAACTCTGCCGCTA-3′ and 5′-TGAGTTACTAGGGCGTCG-3′ (Heck et al., 2003).

Quantification of SA

Whole rosette leaves were collected from 4-week-old soil-grown plants, weighed, and frozen in liquid nitrogen. Three hundred milligrams of frozen tissue was ground in liquid nitrogen, after which, 6 mL of cold methanol was added as an extraction solvent. Twenty microliters of 0.15 mM 3,4,5-trimethoxytranscinnamic acid, dissolved in methanol, was added as an internal standard. Samples were extracted at 4°C for 24 h with mild shaking, after which, 3.6 mL of water and 3 mL of chloroform were added. After brief vortexing, the samples were kept at 4°C for 12 h. The upper phase was dried in a speed vac, and the residue was redissolved in 100 μL of 65% methanol (v/v). Analysis of SA was accomplished by HPLC-tandem mass spectrometry on an Agilent 1200 system using a Waters Xterra MS C18 column (5 μm, 150- × 2.1-mm i.d.). A binary mobile phase consisting of 50 mM ammonium acetate, pH 7, in water (solvent A) and acetonitrile (solvent B) was used at a flow rate of 0.3 mL min^{-1}. Initial conditions were set at 90:10 (A:B) with a linear gradient to 80:20 from 0 to 3 min, followed by a linear gradient to 30:70 from 3 to 13 min and column reequilibration. Following separation, the column effluent was introduced by negative-mode electrospray ionization into an Agilent 6460 triple quadrupole mass spectrometer. Electrospray ionization capillary voltage was –3.2 kV, nebulizer gas pressure was set at 35 pounds per square inch, drying gas temperature was 325°C, flow rate was 9 L min^{-1}, and fragmentor voltage was set to 85 V. Multiple Reaction Monitoring transitions were 137.0 to 93.0 for SA and 237.2 to 103.1 for the internal standard. Collision energies used were 14 eV for SA and 10 eV for the internal standard. Mass data were collected and analyzed using Agilent MassHunter software (version B.02). SA quantification was accomplished using a standard curve over the range 0.01 to 50 μg mL^{-1}.

ACKNOWLEDGMENTS

We thank Junko Maeda for technical support, Drs. Haibing Yang and Angus Murphy for providing us the pOpON vector, Drs. Trenton Parsell and Mahdi Abu-omar for helping with the gas chromatography-flame ionization detector used in DFRC analysis, and Dr. Bruce Cooper for assistance in SA analysis.

Received September 27, 2013; accepted December 19, 2013; published December 31, 2013.

LITERATURE CITED

Abdulrazzak N, Pollet B, Ehlting J, Larsen K, Asnaghi C, Ronseau S, Proux C, Erhardt M, Seltzer V, Renou JP, et al (2006) A coumaroyl-ester-3-hydroxylase insertion mutant reveals the existence of nonredundant meta-hydroxylation pathways and essential roles for phenolic precursors in cell expansion and plant growth. Plant Physiol **140:** 30–48

Altamura MM, Possenti M, Matteucci A, Baima S, Ruberti I, Morelli G (2001) Development of the vascular system in the inflorescence stem of Arabidopsis. New Phytol **151:** 381–389

Beemster GT, De Veylder L, Vercruysse S, West G, Rombaut D, Van Hummelen P, Galichet A, Gruissem W, Inzé D, Vuylsteke M (2005) Genome-wide analysis of gene expression profiles associated with cell cycle transitions in growing organs of Arabidopsis. Plant Physiol **138:** 734–743

Besseau S, Hoffmann L, Geoffroy P, Lapierre C, Pollet B, Legrand M (2007) Flavonoid accumulation in *Arabidopsis* repressed in lignin synthesis affects auxin transport and plant growth. Plant Cell **19:** 148–162

Binns AN, Chen RH, Wood HN, Lynn DG (1987) Cell division promoting activity of naturally occurring dehydrodiconiferyl glucosides: do cell wall components control cell division? Proc Natl Acad Sci USA **84:** 980–984

Bonawitz ND, Chapple C (2010) The genetics of lignin biosynthesis: connecting genotype to phenotype. Annu Rev Genet **44:** 337–363

Bonawitz ND, Chapple C (2013) Can genetic engineering of lignin deposition be accomplished without an unacceptable yield penalty? Curr Opin Biotechnol **24:** 336–343

Bowling SA, Guo A, Cao H, Gordon AS, Klessig DF, Dong X (1994) A mutation in *Arabidopsis* that leads to constitutive expression of systemic acquired resistance. Plant Cell **6:** 1845–1857

Brown DM, Zeef LA, Ellis J, Goodacre R, Turner SR (2005) Identification of novel genes in *Arabidopsis* involved in secondary cell wall formation using expression profiling and reverse genetics. Plant Cell **17:** 2281–2295

Chapple CC, Vogt T, Ellis BE, Somerville CR (1992) An *Arabidopsis* mutant defective in the general phenylpropanoid pathway. Plant Cell **4:** 1413–1424

Coe EH, McCormick SM, Modena SA (1981) White pollen in maize. J Hered **72:** 318–320

Coleman HD, Samuels AL, Guy RD, Mansfield SD (2008) Perturbed lignification impacts tree growth in hybrid poplar—a function of sink strength, vascular integrity, and photosynthetic assimilation. Plant Physiol **148:** 1229–1237

Cosgrove DJ (2005) Growth of the plant cell wall. Nat Rev Mol Cell Biol **6:** 850–861

Craft J, Samalova M, Baroux C, Townley H, Martinez A, Jepson I, Tsiantis M, Moore I (2005) New pOp/LhG4 vectors for stringent glucocorticoid-dependent transgene expression in Arabidopsis. Plant J **41:** 899–918

Czechowski T, Stitt M, Altmann T, Udvardi MK, Scheible WR (2005) Genome-wide identification and testing of superior reference genes for transcript normalization in Arabidopsis. Plant Physiol **139:** 5–17

Delaney TP, Uknes S, Vernooij B, Friedrich L, Weymann K, Negrotto D, Gaffney T, Gut-Rella M, Kessmann H, Ward E, et al (1994) A central role of salicylic acid in plant disease resistance. Science **266:** 1247–1250

Dharmawardhana DP, Ellis BE, Carlson JE (1992) Characterization of vascular lignification in *Arabidopsis thaliana*. Can J Bot **70:** 2238–2244

Dixon RA, Paiva NL (1995) Stress-induced phenylpropanoid metabolism. Plant Cell **7:** 1085–1097

Elkind Y, Edwards R, Mavandad M, Hedrick SA, Ribak O, Dixon RA, Lamb CJ (1990) Abnormal plant development and down-regulation of phenylpropanoid biosynthesis in transgenic tobacco containing a heterologous phenylalanine ammonia-lyase gene. Proc Natl Acad Sci USA **87:** 9057–9061

Fini A, Brunetti C, Di Ferdinando M, Ferrini F, Tattini M (2011) Stress-induced flavonoid biosynthesis and the antioxidant machinery of plants. Plant Signal Behav **6:** 709–711

Franke R, Hemm MR, Denault JW, Ruegger MO, Humphreys JM, Chapple C (2002a) Changes in secondary metabolism and deposition of an unusual lignin in the ref8 mutant of Arabidopsis. Plant J **30:** 47–59

Franke R, Humphreys JM, Hemm MR, Denault JW, Ruegger MO, Cusumano JC, Chapple C (2002b) The Arabidopsis *REF8* gene encodes the 3-hydroxylase of phenylpropanoid metabolism. Plant J **30:** 33–45

Franke R, McMichael CM, Meyer K, Shirley AM, Cusumano JC, Chapple C (2000) Modified lignin in tobacco and poplar plants over-expressing the Arabidopsis gene encoding ferulate 5-hydroxylase. Plant J **22:** 223–234

Gallego-Giraldo L, Escamilla-Trevino L, Jackson LA, Dixon RA (2011) Salicylic acid mediates the reduced growth of lignin down-regulated plants. Proc Natl Acad Sci USA **108:** 20814–20819

Heck S, Grau T, Buchala A, Métraux JP, Nawrath C (2003) Genetic evidence that expression of NahG modifies defence pathways independent of salicylic acid biosynthesis in the Arabidopsis-*Pseudomonas syringae* pv. *tomato* interaction. Plant J **36:** 342–352

Hoffmann L, Besseau S, Geoffroy P, Ritzenthaler C, Meyer D, Lapierre C, Pollet B, Legrand M (2004) Silencing of hydroxycinnamoyl-coenzyme A shikimate/quinate hydroxycinnamoyltransferase affects phenylpropanoid biosynthesis. Plant Cell **16:** 1446–1465

Huang J, Gu M, Lai Z, Fan B, Shi K, Zhou YH, Yu JQ, Chen Z (2010) Functional analysis of the Arabidopsis PAL gene family in plant growth, development, and response to environmental stress. Plant Physiol **153:** 1526–1538

Jones L, Ennos AR, Turner SR (2001) Cloning and characterization of irregular xylem4 (*irx4*): a severely lignin-deficient mutant of Arabidopsis. Plant J **26:** 205–216

Landry LG, Chapple CC, Last RL (1995) Arabidopsis mutants lacking phenolic sunscreens exhibit enhanced ultraviolet-B injury and oxidative damage. Plant Physiol **109:** 1159–1166

Lee J, Nam J, Park HC, Na G, Miura K, Jin JB, Yoo CY, Baek D, Kim DH, Jeong JC, et al (2007) Salicylic acid-mediated innate immunity in Arabidopsis is regulated by SIZ1 SUMO E3 ligase. Plant J **49:** 79–90

Leplé JC, Dauwe R, Morreel K, Storme V, Lapierre C, Pollet B, Naumann A, Kang KY, Kim H, Ruel K, et al (2007) Downregulation of cinnamoyl-coenzyme A reductase in poplar: multiple-level phenotyping reveals effects on cell wall polymer metabolism and structure. Plant Cell **19:** 3669–3691

Li X, Bonawitz ND, Weng JK, Chapple C (2010) The growth reduction associated with repressed lignin biosynthesis in *Arabidopsis thaliana* is independent of flavonoids. Plant Cell **22:** 1620–1632

Li X, Clarke JD, Zhang Y, Dong X (2001) Activation of an EDS1-mediated R-gene pathway in the *snc1* mutant leads to constitutive, NPR1-independent pathogen resistance. Mol Plant Microbe Interact **14:** 1131–1139

Li X, Weng JK, Chapple C (2008) Improvement of biomass through lignin modification. Plant J **54:** 569–581

Livak KJ, Schmittgen TD (2001) Analysis of relative gene expression data using real-time quantitative PCR and the $2^{-\Delta\Delta C_T}$ method. Methods **25:** 402–408

Lu FC, Ralph J (1997) Derivatization followed by reductive cleavage (DFRC method), a new method for lignin analysis: protocol for analysis of DFRC monomers. J Agric Food Chem **45:** 2590–2592

Lynn DG, Chen RH, Manning KS, Wood HN (1987) The structural characterization of endogenous factors from *Vinca rosea* crown gall tumors that promote cell division of tobacco cells. Proc Natl Acad Sci USA **84:** 615–619

Marcinowski S, Grisebach H (1977) Turnover of coniferin in pine seedlings. Phytochemistry **16:** 1665–1667

Mauch-Mani B, Slusarenko AJ (1996) Production of salicylic acid precursors in a major function of phenylalanine ammonia-lyase in the resistance of *Arabidopsis* to *Peronospora parasitica*. Plant Cell **8:** 203–212

Meyer K, Shirley AM, Cusumano JC, Bell-Lelong DA, Chapple C (1998) Lignin monomer composition is determined by the expression of a cytochrome P450-dependent monooxygenase in Arabidopsis. Proc Natl Acad Sci USA **95:** 6619–6623

Mo YY, Nagel C, Taylor LP (1992) Biochemical complementation of chalcone synthase mutants defines a role for flavonols in functional pollen. Proc Natl Acad Sci USA **89:** 7213–7217

Mol J, Grotewold E, Koes R (1998) How genes paint flowers and seeds. Trends Plant Sci **3:** 212–217

Moore I, Samalova M, Kurup S (2006) Transactivated and chemically inducible gene expression in plants. Plant J **45:** 651–683

Mündermann L, Erasmus Y, Lane B, Coen E, Prusinkiewicz P (2005) Quantitative modeling of Arabidopsis development. Plant Physiol **139:** 960–968

O'Connell A, Holt K, Piquemal J, Grima-Pettenati J, Boudet A, Pollet B, Lapierre C, Petit-Conil M, Schuch W, Halpin C (2002) Improved paper pulp from plants with suppressed cinnamoyl-CoA reductase or cinnamyl alcohol dehydrogenase. Transgenic Res **11:** 495–503

Orr JD, Lynn DG (1992) Biosynthesis of dehydrodiconiferyl alcohol glucosides: implications for the control of tobacco cell growth. Plant Physiol **98:** 343–352

Pallas JA, Paiva NL, Lamb C, Dixon RA (1996) Tobacco plants epigenetically suppressed in phenylalanine ammonia-lyase expression do not develop systemic acquired resistance in response to infection by tobacco mosaic virus. Plant J **10:** 281–293

Persson S, Caffall KH, Freshour G, Hilley MT, Bauer S, Poindexter P, Hahn MG, Mohnen D, Somerville CR (2007) The *Arabidopsis irregular xylem8* mutant is deficient in glucuronoxylan and homogalacturonan, which are essential for secondary cell wall integrity. Plant Cell **19:** 237–255

Petersen M, Brodersen P, Naested H, Andreasson E, Lindhart U, Johansen B, Nielsen HB, Lacy M, Austin MJ, Parker JE, et al (2000) Arabidopsis map kinase 4 negatively regulates systemic acquired resistance. Cell **103:** 1111–1120

Petersen PD, Lau J, Ebert B, Yang F, Verhertbruggen Y, Kim JS, Varanasi P, Suttangkakul A, Auer M, Loqué D, et al (2012) Engineering of plants with improved properties as biofuels feedstocks by vessel-specific complementation of xylan biosynthesis mutants. Biotechnol Biofuels **5:** 84

Pinçon G, Maury S, Hoffmann L, Geoffroy P, Lapierre C, Pollet B, Legrand M (2001) Repression of *O*-methyltransferase genes in transgenic tobacco affects lignin synthesis and plant growth. Phytochemistry **57:** 1167–1176

Piquemal J, Lapierre C, Myton K, O'Connell A, Schuch W, Grima-Pettenati J, Boudet AM (1998) Down-regulation of cinnamoyl-CoA reductase induces significant changes of lignin profiles in transgenic tobacco plants. Plant J **13:** 71–83

Poethig RS (2003) Phase change and the regulation of developmental timing in plants. Science **301:** 334–336

Pouteau S, Albertini C (2009) The significance of bolting and floral transitions as indicators of reproductive phase change in Arabidopsis. J Exp Bot **60:** 3367–3377

Reddy MS, Chen F, Shadle G, Jackson L, Aljoe H, Dixon RA (2005) Targeted down-regulation of cytochrome P450 enzymes for forage quality improvement in alfalfa (*Medicago sativa* L.). Proc Natl Acad Sci USA **102:** 16573–16578

Rohde A, Morreel K, Ralph J, Goeminne G, Hostyn V, De Rycke R, Kushnir S, Van Doorsselaere J, Joseleau JP, Vuylsteke M, et al (2004) Molecular phenotyping of the pal1 and pal2 mutants of *Arabidopsis thaliana* reveals far-reaching consequences on phenylpropanoid, amino acid, and carbohydrate metabolism. Plant Cell **16:** 2749–2771

Ruegger M, Meyer K, Cusumano JC, Chapple C (1999) Regulation of ferulate-5-hydroxylase expression in Arabidopsis in the context of sinapate ester biosynthesis. Plant Physiol **119:** 101–110

Ruuhola TM, Julkunen-Tiitto MR (2000) Salicylates of intact *Salix myrsinifolia* plantlets do not undergo rapid metabolic turnover. Plant Physiol **122:** 895–905

Schilmiller AL, Stout J, Weng JK, Humphreys J, Ruegger MO, Chapple C (2009) Mutations in the cinnamate 4-hydroxylase gene impact metabolism, growth and development in Arabidopsis. Plant J **60:** 771–782

Shadle G, Chen F, Srinivasa Reddy MS, Jackson L, Nakashima J, Dixon RA (2007) Down-regulation of hydroxycinnamoyl CoA: shikimate hydroxycinnamoyl transferase in transgenic alfalfa affects lignification, development and forage quality. Phytochemistry **68:** 1521–1529

Strack D, Sharma V (1985) Vacuolar localization of the enzymatic synthesis of hydroxycinnamic acid esters of malic acid in protoplasts from *Raphanus sativus* leaves. Physiol Plant **65:** 45–50

Taylor LP, Jorgensen R (1992) Conditional male-fertility in chalone synthase-deficient petunia. J Hered **83:** 11–17

Teutonico RA, Dudley MW, Orr JD, Lynn DG, Binns AN (1991) Activity and accumulation of cell division-promoting phenolics in tobacco tissue cultures. Plant Physiol **97:** 288–297

Turner SR, Somerville CR (1997) Collapsed xylem phenotype of *Arabidopsis* identifies mutants deficient in cellulose deposition in the secondary cell wall. Plant Cell **9:** 689–701

Ullah H, Chen JG, Wang S, Jones AM (2002) Role of a heterotrimeric G protein in regulation of Arabidopsis seed germination. Plant Physiol **129:** 897–907

Vanholme R, Cesarino I, Rataj K, Xiao Y, Sundin L, Goeminne G, Kim H, Cross J, Morreel K, Araujo P, et al (2013) Caffeoyl shikimate esterase (CSE) is an enzyme in the lignin biosynthetic pathway in Arabidopsis. Science **341:** 1103–1106

Weng JK, Akiyama T, Bonawitz ND, Li X, Ralph J, Chapple C (2010) Convergent evolution of syringyl lignin biosynthesis via distinct pathways in the lycophyte *Selaginella* and flowering plants. Plant Cell **22:** 1033–1045

Wielopolska A, Townley H, Moore I, Waterhouse P, Helliwell C (2005) A high-throughput inducible RNAi vector for plants. Plant Biotechnol J **3:** 583–590

Yang F, Mitra P, Zhang L, Prak L, Verhertbruggen Y, Kim JS, Sun L, Zheng K, Tang K, Auer M, et al (2013) Engineering secondary cell wall deposition in plants. Plant Biotechnol J **11:** 325–335